Importance of convection in the compaction mechanisms of anisotropic granular media

Philippe Ribière, Patrick Richard, Renaud Delannay, and Daniel Bideau
Groupe Matière Condensée et Matériaux, UMR CNRS 6626, Université de Rennes 1, Campus de Beaulieu, F-35042 Rennes Cedex, France

(Received 22 July 2004; revised manuscript received 22 October 2004; published 25 January 2005)

We report the experimental observation of vortex patterns in a vertically tapped granular media. Depending on the tapping acceleration, two behaviors are observed. For high acceleration a convection vortex appears in the whole media, whereas for low acceleration two unstable vortices appear in the upper part of the media and slowly compact the lower part. We explain the formation of the vortices and relate them to granular convection. Our results demonstrate the importance of compression wave propagation on granular compaction.

DOI: 10.1103/PhysRevE.71.011304 PACS number(s): 45.70.Cc, 45.70.Mg, 83.80.Fg

In hydrodynamics, flow instabilities lead to the formation of vortex patterns which affect the behavior of the fluid. It is well known that granular media can exhibit both fluidlike and a solidlike behavior and thus do not behave like classical fluids. In order to understand the specificities of granular media, some studies of instabilities have been carried out for vertical vibrated granular layers [1–3], granular flows [4–6], and gazes [7]. Moreover, a granular packing under vertical shaking leads to a global compaction [9–11], and this compaction can be linked to convection [10,12,13]. Since convection in fluids can lead to instabilities, can granular systems under compaction exhibit vortices? In this paper we present a vortex creation process that occurs in a tapped pile of anisotropic grains and explain the mechanisms of such a creation. Since it has been recently proved that grain anisotropy is important in pattern formation [3] we focus on anisotropic granular materials.

The experimental set up consists of a glass cylinder of diameter $D \approx 10$ cm filled with 600 g of grains (corresponding to a height of roughly 10 cm). This container is placed on a plate connected to an electromagnetic exciter (LDS V406) which induces a vertical displacement of the plate. The container is, in this way, regularly shaken ($\Delta t = 1s$) by vertical taps. Each tap is created by one entire period of sine wave at a fixed frequency $f = 30$ Hz. The resulting motion of the whole system, monitored by an accelerometer at the bottom of the container, is, however, more complicated than a simple sine wave. At first, the system undergoes a positive acceleration followed by a negative peak with a minimum, $-\gamma_{max}$. After the applied voltage stops, the system relaxes to its normal repose position. This negative peak acceleration is used to characterize the tap intensity by the dimensionless acceleration $\Gamma = \gamma_{max}/g$ (with $g = 9.81$ m s^{-2}). It should be pointed out that we only used taps for which the grains took off from the bottom of the glass cylinder, i.e., above the lift-off threshold. The packing fraction is measured using a γ-ray absorption set up [10]. The results presented here have been obtained using long rice (basmati rice). In order to quantify the anisotropy, each grain is assimilated to an ellipsoid. The mean ratio between the two axes is 2.5 with 10% of dispersion. The length of the longer axis will be noted d. The method used to build our initial packing, already used for spheres [10], is reproducible (we obtain the same initial packing fraction $\Phi \approx 0.56$ and the same packing fraction evolution for a given Γ). Sequences of 10^4–10^6 taps are carried out. The only control parameter is the tapping intensity Γ. Here we call "time" the number of taps and the "dynamics" is the succession of static equilibrium induced by the taps. The mean packing fraction increases monotically with time following stretched exponential. All the details on the compaction dynamics can be found elsewhere [12].

The first observation is that convection takes place in the medium: after τ_{app}, a given time depending on Γ, one or two counterrotating vertical convection rolls appear. They are easily identified by tracking a grain's position after each tap. To characterize them, we measure the time it takes a grain to revolve around the center of the roll, τ_{conv}. Figure 1(a) reports the variations of τ_{conv} and τ_{app} with Γ. As expected, the greater the tapping acceleration is, the smaller these two times are. Concerning the number of rolls, two cases should be considered. For high tapping intensity (typically $\Gamma > 3$) convection takes place within the whole medium. After about ten taps, two convection rolls appear but this situation becomes unstable. One of the rolls progressively disappears and after this transient the whole medium is occupied by only one roll and the free surface of the medium is tilted from the horizontal (for example, about 20° for $\Gamma = 6$). A sketch and a snapshot of this convection roll is reported in Fig. 1(b). The arrows represent in arbitrary units the displacement field of the grains and clearly demonstrate the existence of convection. A radial displacement profile is reported Fig. 1(c). An immobile core can be observed. In an ideal system this nonmobile part should be reduced to a point, but due to the formation of spatially correlated clusters the size obtained is around $4d$. After this part a linear profile is found with a slope compatible with the value of τ_{conv}. This part of the packing rotates around the immobile core like a solid. For lower values of the tapping intensity (typically $\Gamma < 3$) two convection rolls roughly equally sized and localized near the free surface appear. The other part of this packing (below the rolls) is not submitted to convection. As for the high tapping intensity case, this situation is unstable. Contrary to the previous case the two rolls do not merge: their size continuously decreases until they totally disappear. Note that the convection turns out not to be a phenomenon in competition with compaction. On the contrary, the convection rolls create at their base a band of high packing fraction.

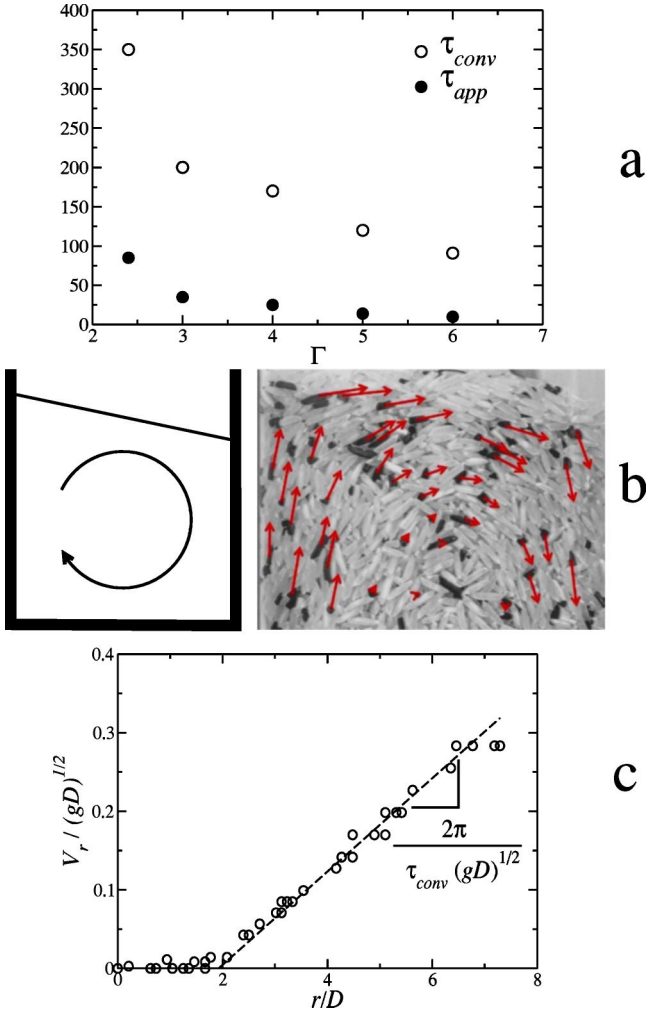

FIG. 1. (a) τ_{app} and τ_{conv} (see text for definition) vs tapping intensity Γ. (b) Sketch of the convection obtained for basmati rice and for Γ=6 (left-hand side) and snapshot of the medium during relaxation (right-hand side) where convection roll can be clearly seen on the walls. (c) Radial displacement profile: the granular medium rotates like a solid around an immobile core.

On Fig. 2(a) taken for Γ=2.4 after 1500 taps, this band is clearly visible at the base of the two convection rolls and one can observe that the grains in this band have a preferential horizontal orientation, due to the motion of the rice in convection. The band of high density can be distinguished on the packing fraction profile [Fig. 2(b)]. The convection rolls create the high-density zone and their size decrease corresponds to the growth of this zone. The orientation of the grains is totally different from the one observed in another compaction experiment [14]. Indeed, the vessel used in [14] is very narrow (one grain length) compared to ours (about 20 grain lengths). Thus, the nematic ordering observed in this tube is likely due to the strong confinement and no convection is possible [3]. Note that the aspect ratio of the grains is probably also an important parameter.

To understand the convection creation and evolution we have used a high-speed camera (1000 images per second) to analyze the motion and the deformation of the packing dur-

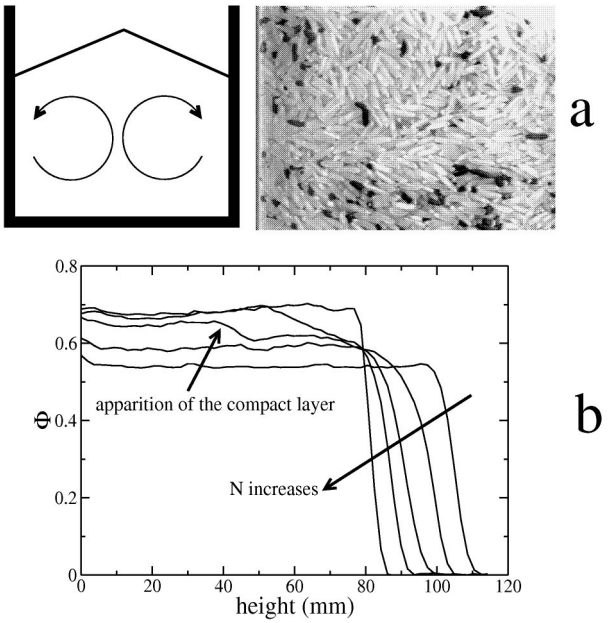

FIG. 2. (a) Sketch of the convection obtained for basmati rice and for Γ=2.4 (left) and snapshot of the medium during relaxation (right). The compact zone can be observed on the sidewalls. (b) Packing fraction profile obtained for basmati rice at Γ=2.4 for various number of taps (see the arrow): N=0, 10, 100, 3116, 100 00, 311 62, and 100 000.

ing a tap. Four phases can be visually distinguished (see Fig. 3):

(a) the rice follows the motion of the plate (phase 1);

(b) the rice takes off from the bottom (phase 2);

(c) the rice lands on the bottom (phase 3);

(d) a compression wave propagates throughout the medium (phase 4).

The rate of compaction and dilatation is measured during each phase for the first tap (the motion of the grains is greater here than during the other solicitations and thus the detection of motion is easier. The data were averaged on two different experiments and no significant differences were observed. To track the grains, we use an image processing software that computes the gray level profile along a vertical line at the sidewall. For clarity each profile is reported in the reference frame of the vessel. To improve contrast and thus to have sharp peaks on the gray level profile, 8% of the grains are

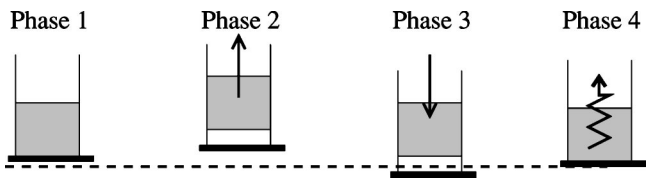

FIG. 3. Sketch of the four phases of a tap. The dashed line corresponds to the repose position of the vessel. The medium follow the motion of the vessel (phase 1), takes off from the bottom (phase 2), lands on the bottom (phase 3), and finally the compression wave propagates (phase 4).

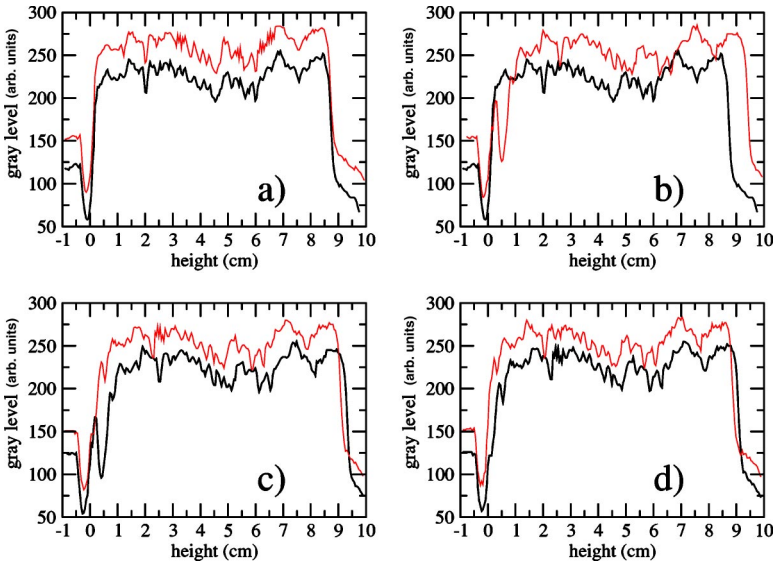

FIG. 4. Gray level profiles along a vertical line on the picture of the system for $\Gamma=6$: (a) before (down) and after (up) the first tap, (b) just before the medium takes off (down) and at its higher position, (c) at its higher position (down) and just after the medium lands (up), (d) just before (down) and after the compression wave. For clarity, each curve has an offset in the *y* axis and is reported in the reference frame of the vessel.

painted in black. We can then follow the displacement of the peaks between each picture (1000 pictures per seconds) and thus detect dilatation, compaction, or wave propagation during each phase of the motion. The precision on the peak displacement is 0.3 mm for a packing height of about 10 cm. Note that, in order to avoid overlapping, each profile presented here is shifted vertically. On Fig. 4(a), the two gray level profiles correspond, respectively, to the state before and after the first tap of $\Gamma=6$. These two profiles are similar and the peaks present can be easily tracked. Let us now examine with this method the phases of the motion. During the first phase, the rice follows the motion of the container. As the medium is in a stable configuration, this motion does not create a relative displacement of the grains. As the cylinder slows down, the medium takes off from the bottom and a dilatation of the piling is observed [Fig. 4(b)]. This dilatation is not uniform: 1 mm for the upper part of the packing and 0.5 mm for the lower part. A study of the orientation of the grains during this phase shows that they have a tendency to align vertically. Moreover, as already observed for glass beads in [13], all the packing takes off and its bottom is still parallel to the plate. During the third phase [Fig. 4(c)], the rice lands, which induces a compaction of the medium. Surprisingly, this compaction is smaller than the dilatation monitored during the second phase and at this stage the medium is less compact than initially. Note that the vertical orientation tendency of the rice always exists even if it is less visible than during the second phase. In fact, the medium mainly compacts during the last phase (propagation of the compression wave). The evolution of the gray level during that phase is reported in Fig. 4(d) and compaction of the medium is indeed observed. The compression wave can be easily tracked on the fast camera movie. Its velocity can then be measured. For $\Gamma=6$ we have $V\approx 16.5\ m\ s^{-1}$. Moreover, it is only during this phase of propagation that the contribution to convection appears. Indeed, during phases 1–3 the bottom of the packing remains parallel to the plate, hence no convectionlike grain motions are observed. This result clearly demonstrates that compaction and convection are strongly linked. The compression wave is a consequence of the dissipation of the interaction energy stored by the grains during the previous motion phases. This allows the grains to move slightly around their initial position and to possibly find a more stable position corresponding to a higher value of the packing fraction. The velocity of the compression wave is of the same order of magnitude as that obtained in the same set up with glass beads [13] but smaller than the values obtained in a one-dimensional granular medium [8].

It should be pointed out that in our set up, compaction is mainly associated with compression, wave propagation, and convection. Nevertheless, it is not the only one, since compaction can be observed even without convection [9]. This also explains why the characteristic times found in [10] are smaller than those obtained in [9].

For $\Gamma=6$, the effect of the compression wave is easy to analyze for two reasons. First, the dilatation of the medium just before the wave is still important and its effect is easier to appreciate. Second, the intensity of the compression wave is high because the medium lands on the plate when the plate comes up again.

We have also performed such an analysis for $\Gamma=2.4$. In Fig. 5(a), the two gray level profiles reported correspond, respectively, to the state before and after the first tap. The motion of the grains is smaller than for $\Gamma=6$. Many characteristics of the medium motion are similar to those obtained for $\Gamma=6$. During the first phase (the grains follow the plate motion) the medium is not affected. During the second phase, we monitor a small dilatation in the medium. Nevertheless, the mean orientation does not change as much as for $\Gamma=6$. During the third phase, the packing fraction increases. What is surprising and different from the $\Gamma=6$ case is that during the last phase, the compression wave propagates inhomogeneously through the medium. Indeed, no motion is visible at the bottom, whereas a small displacement of 1 mm is monitored on the top of the packing. This is in agreement with previous analysis: the wave does not affect the bottom part of the packing where no convection is observed, contrary to the upper part where both convection and compression wave propagation are present. Note that, as expected, the effect of the compression wave is less important for $\Gamma=2.4$ than for $\Gamma=6$.

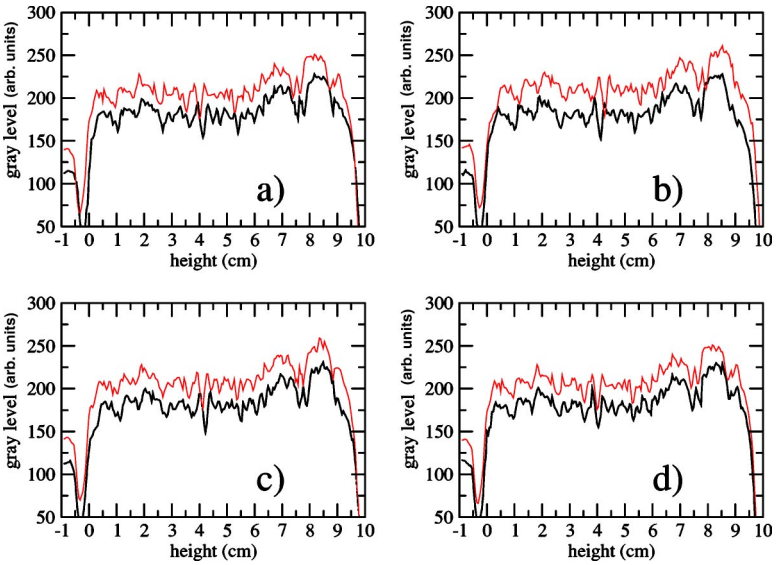

FIG. 5. Gray level profiles along a vertical line on the picture of the system for $\Gamma = 2.4$: (a) before (down) and after the first tap (up), (b) just before the medium take off (down) and at its higher position (up), (c) at its higher position (down) and just after the medium lands (up), (d) just before (down) and after (up) the compression wave. For clarity, each curve has an offset in the *y* axis and is reported in the reference frame of the vessel.

We explain this behavior difference by the motion of the packing relative to the bottom plate. For $\Gamma = 2.4$, the medium lands as the plate is moving downwards. Therefore, the apparent fall velocity of the medium is smaller than in the motionless case and the intensity of the compression wave is smaller than for $\Gamma = 6$. The other observation is that there is also a strong correlation between the apparition of convection and of the compression wave. Indeed, in all our experiments the compression wave creates a motion only in the part of the medium where convection will take place during the other solicitations. This explanation helps understanding the transition between the two behaviors: for $\Gamma = 3$, the fall of the medium coincides with the motionless, lowest position of the plate.

To summarize, the unique instability presented in this paper leads to a vortices formation during compaction of anisotropic granular media at relatively low tapping intensity. Below the vortices, an ordered compact zone can be created where the grains are oriented horizontally. By analyzing the packing behavior during one tap we showed that the main compaction mechanism is due to a compression wave propagation. Furthermore, this compression wave propagation creates convection proving the strong correlation between granular compaction and convection.

[1] P. Evesque and J. Rajchenbach, Phys. Rev. Lett. **62**, 44 (1989).
[2] P. B. Umbanhowar, F. Melo, and H. L. Swinney, Nature (London) **382**, 793 (1996).
[3] D. L. Blair, T. Neicu, and A. Kudrolli, Phys. Rev. E **67**, 031303 (2003).
[4] M. Y. Louge and S. C. Keast, Phys. Fluids **13**, 1213 (2001).
[5] O. Pouliquen, J. Delour, and S. B. Savage, Nature (London) **386**, 816 (1997).
[6] Y. Forterre and O. Pouliquen, Phys. Rev. Lett. **86**, 5886 (2001).
[7] E. Falcon, R. Wunenburger, P. Evesque, S. Fauve, C. Chabot, Y. Garrabos, and D. Beysens, Phys. Rev. Lett. **83**, 440 (1999).
[8] E. Falcon, Ph.D. thesis, Lyon, 1997 (unpublished).
[9] J. B. Knight, C. G. Fandrich, C. N. Lau, H. M. Jaeger, and S. R. Nagel, Phys. Rev. E **51**, 3957 (1995); E. R Nowak, J. B. Knight, E. Ben-Naim, H. M. Jaeger, and S. R. Nagel, *ibid.* **57**, 1971 (1998).
[10] P. Philippe and D. Bideau, Europhys. Lett. **60**, 677 (2002).
[11] P. Richard, P. Philippe, F. Barbe, S. Bourlès, X. Thibault, and D. Bideau, Phys. Rev. E **68**, 020301(R) (2003).
[12] P. Ribière, P. Richard, D. Bideau, and R. Delannay (unpublished).
[13] P. Philippe and D. Bideau, Phys. Rev. Lett. **91**, 104302 (2003).
[14] F. X. Villarruel, B. E. Lauderdale, D. M. Mueth, and H. M. Jaeger, Phys. Rev. E **61**, 6914 (2000).